Wind Engineering Joint Usage/Research Center
FY2022 Research Result Report

Research Field: Wind Hazard Mitigation/Wind Resistant design
Research Year: FY2022
Research Number: 22223002
Research Theme: Wind pressure characteristics of retractable dome roofs depending on various wind environments

Representative Researcher: Sung Won, Yoon

Budget [FY2022]: 280000Yen

*There is no limitation of the number of pages of this report.
*Figures can be included to the report and they can also be colored.
*Submitted reports will be uploaded to the JURC Homepage.

1. Research Aim

There are relatively fewer studies on wind load for retractable dome roofs than for general dome roofs, and a wind load code has yet to be established. Therefore, research on retractable dome roofs has been conducted jointly with the Wind Engineering Research Center Joint Usage/Research Center since 2018. Previous studies have focused on the shape of the roof, the retractable type, the opening ratio, the height-span ratio (hereafter called as h/D), and the rise-span ratio (hereafter called as f/D). However, in the previous research, only one airflow condition corresponding to flat terrain category Ⅱ (power law(α) = 0.15) of the Japanese wind load code was considered. The distribution of wind pressure on a dome roof varies according to the changes in velocity and turbulence intensity, which are characteristics of airflow. Lee et al. (2021) investigated the distribution of wind pressure for closed and retractable dome roofs considering various airflow conditions (power law(α) = 0.21 and 0.33). They confirmed that the change in airflow conditions affects the change in wind pressure applied to the dome roof, and the higher the power-law exponent(α), the greater the effect of positive pressure. Based on the above results, it can be expected that changes in airflow will have a significant impact on changes in wind pressure of various retractable dome roofs. Therefore, this research aims to analyze the wind pressure characteristics of retractable dome roofs according to the change in airflow conditions.

2. Research Method

2.1 model

This study was conducted on a central open-type dome roof with an opening in the center of the dome, and a total of four models were produced as shown in Fig. 2. The opening ratio and f/D of the model were determined through a case study of the actually constructed retractable dome roof structure. In the case of the opening ratio of actually constructed retractable dome roof, it was found to be composed of 20% to 50% based on the roof area. Therefore, the opening and closing rates of the model were composed of 30%, 50%, and 55%. For f/D, it was configured between 0.00 and 0.18, with an average value of 0.09, close to 0.1. Therefore, the f/D of the model consisted of 0.1 and 0.05. Details of the four models are shown in Fig. 2.2-2.5.

Fig. 2.1 Test models

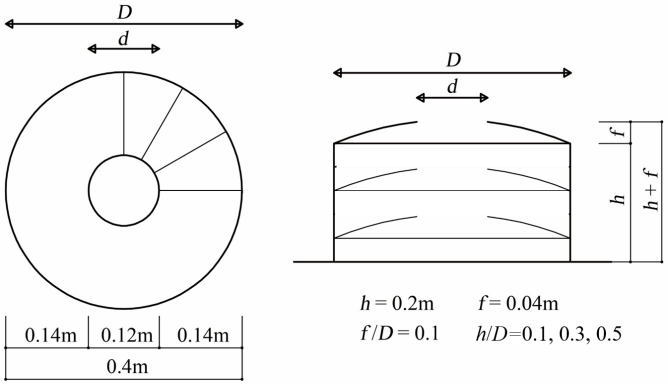

Fig. 2.2 Dimensions of Model I

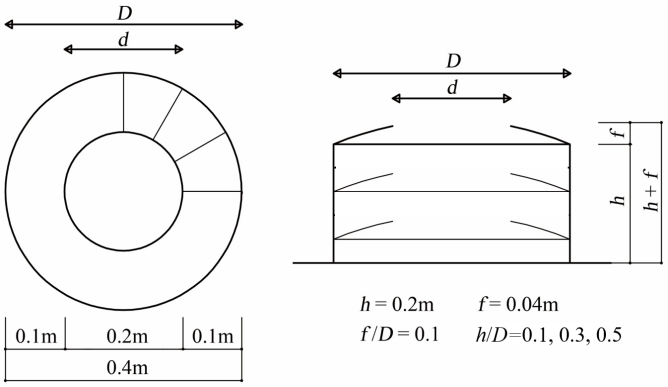

Fig. 2.3 Dimensions of Model II

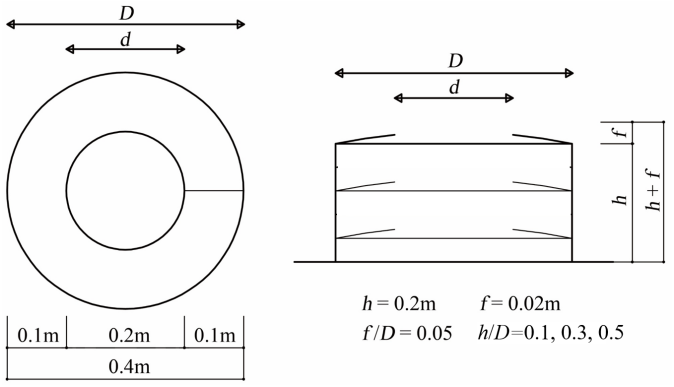

Fig. 2.4 Dimensions of ModelⅢ

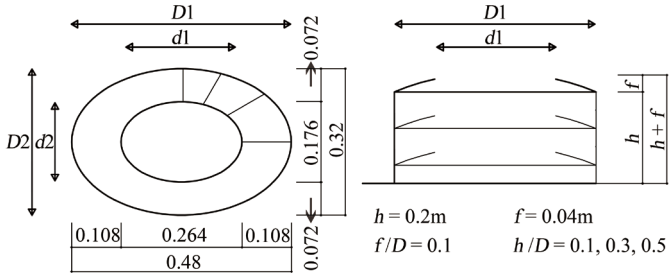

Fig. 2.5 Dimensions of ModelⅣ

2.2 Characteristics of Approaching Oncoming Flow

As for the state of the ground roughness surface for the experiment, a total of three surface roughness Ⅰ, Ⅲ and Ⅳ (α = 0.10, 0.20, 0.27) were reproduced out of the five surface types presented by AIJ-RLB (2015) to compare and analyze the characteristics of wind pressure according to various wind environments.

Fig. 2.6 shows the Profiles of the mean wind speed according to the power-law exponent(α). The dotted line in Figure represents the roof height of the model. At the maximum height $z(h+f)$ = 0.24m of the model roof, the mean wind speed decreases as the power-law exponent(α) increases, with 8.97m/s, 8.86m/s, and 7.26m/s, respectively. Fig. 2.7 shows the profiles of turbulence intensity according to the power-law exponent(α). At the maximum height $z(h+f)$ = 0.24m of the model roof, the turbulence intensity increases as the power-law exponent(α) increases, with 14.3%, 15.4%, and 23.5%, respectively. The power spectrum of the longitudinal wind velocity fluctuation is consistent with the target von Karman spectrum, as shown in Fig. 2.9.

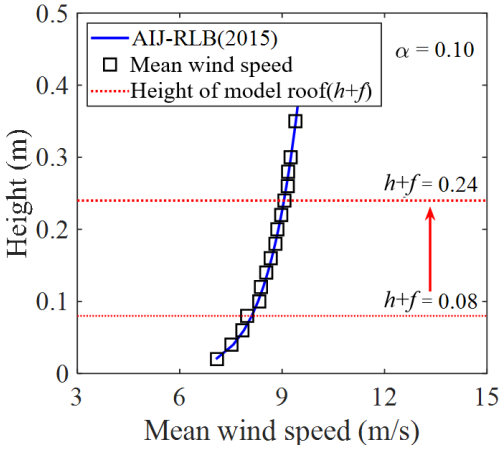

(a) $\alpha = 0.10$

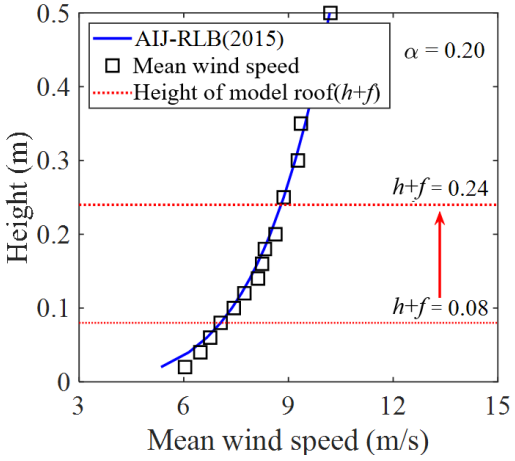

(b) $\alpha = 0.20$

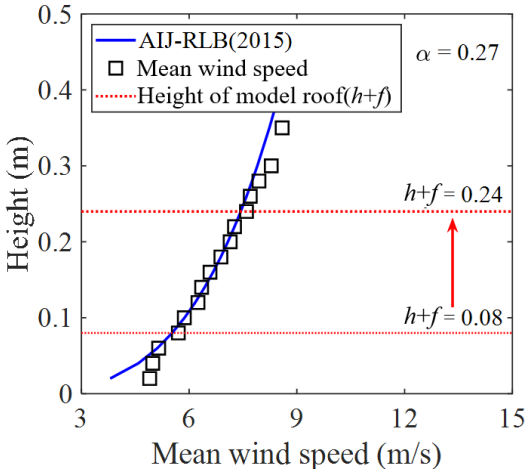

(c) $\alpha = 0.27$

Fig. 2.7 Profiles of turbulence intensity depending on α

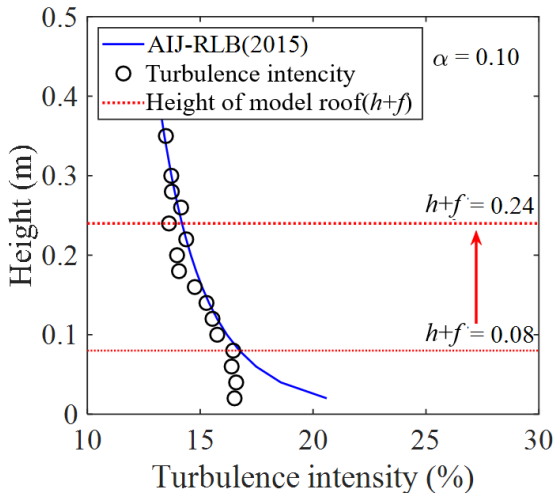

(a) $\alpha = 0.10$

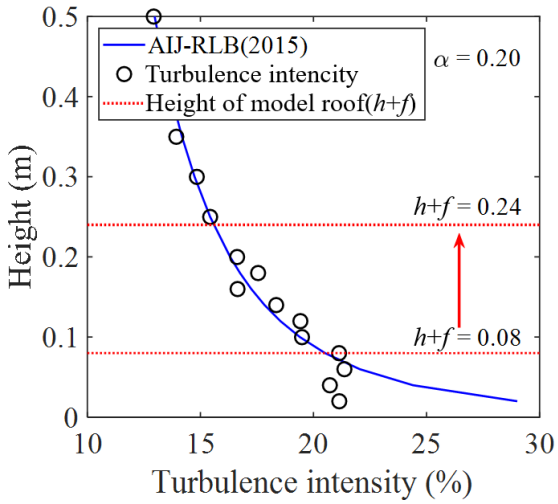

(b) $\alpha = 0.20$

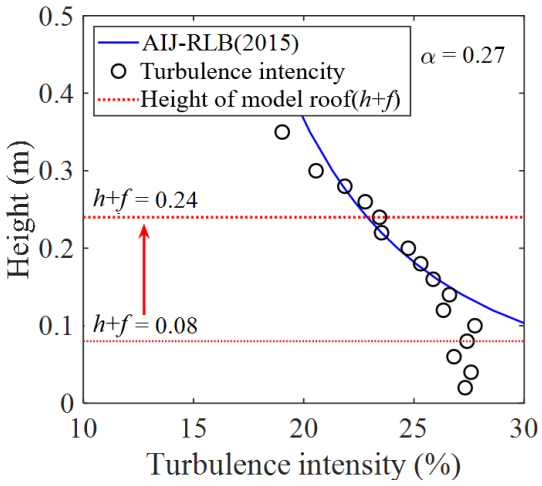

(c) $\alpha = 0.27$

Fig. 2.8 Profiles of turbulence intensity depending on α

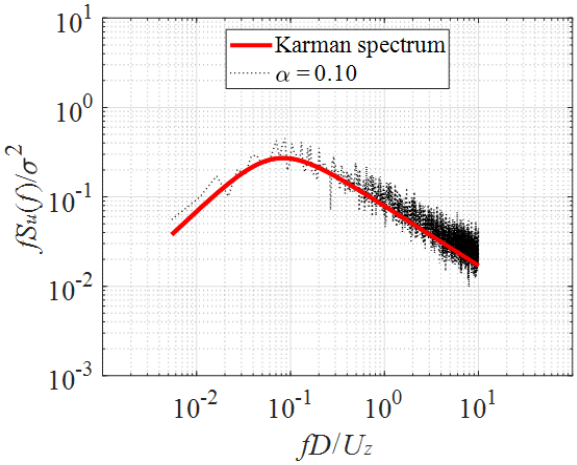

(a) $\alpha = 0.10$

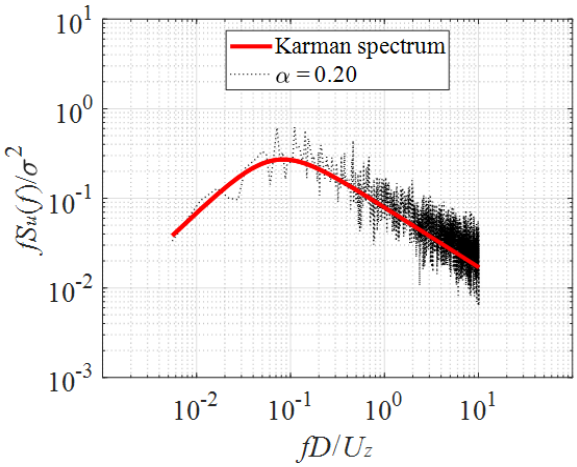

(b) $\alpha = 0.20$

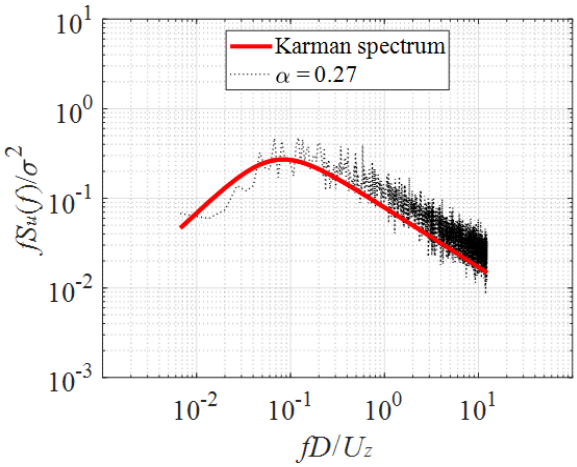

(c) $\alpha = 0.27$

Fig. 2.10 Power spectra of fluctuating wind speed

3. Research Result

3.1 General characteristics of wind pressure distribution

Because all four experimental models used in this study exhibited similar wind pressure distribution characteristics, this report presents the experimental results for Model I.

Fig. 3.1(a) shows the mean pressure coefficient of the external roof surface. In the windward area, the normalized diameter ranged from 0–0.35, and the absolute value and variation in the mean pressure coefficient were similar to those of the closed-dome roof. This is because of the separation that occurs at the windward edge of the roof and the reattachment that occurs at 0.1 of the normalized diameter. Additionally, the magnitude of the absolute value and reattachment distance tended to increase as h/D increased. This was due to the decreasing turbulence intensity in the oncoming flow and the increasing wind speed as the height increased. In the area after reattachment, from normalized diameter 0.1 to 0.35, the absolute values increased gradually owing to the influence of the boundary layer formed on the dome roof surface. The mean pressure coefficient on the leeward side was somewhat larger in absolute value at the roof edge of the open area, with a normalized diameter of 0.65, compared to that of the closed dome roof. This was due to the additional separation of the flow at the roof edge of the open area.

Fig. 3.1(b) shows the fluctuating pressure coefficient. It can be seen that the absolute value is larger than 0.2 at normalized diameters of 0 and 0.65, which are the roof edges of the windward side and open area, respectively, where the separation of the flow occurs, compared to other areas.

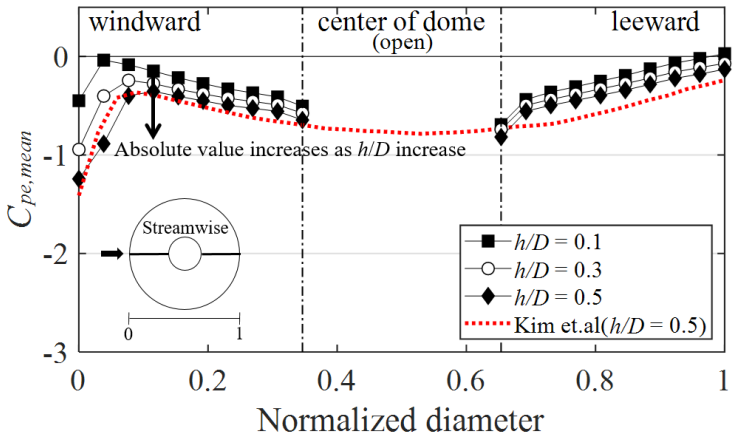

(a) $C_{pe,mean}$

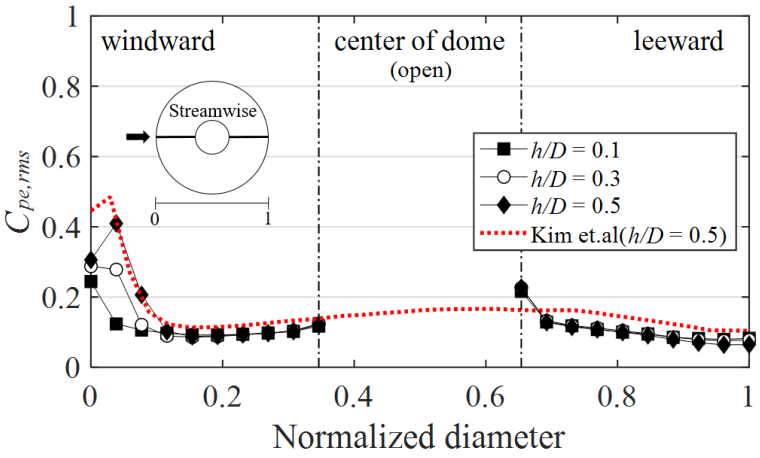

(b) $C_{pe,rms}$

Fig. 3.1 Variation of mean and fluctuating pressure coefficient for the external roof surface of Model I

Fig. 3.2 shows the mean and fluctuating pressure coefficients for the internal roof surface of Model I. By examining the mean pressure coefficient, as shown in Fig. 3.2 (a), we can see that negative pressure is dominant. The dominance of negative pressure on the internal roof surface was due to the inflow of air into the building through the openings and the internal circulation caused by the inflow of air. The windward side is not directly affected by the oncoming flow; therefore, the mean pressure coefficients are similar. However, the roof edge of the open area, which had a normalized diameter of 0.65, had a slightly larger absolute value, similar to that of the external side. This was because it was affected by the vortex caused by the same flow separation as that of the external roof.

Fig. 3.2(b) shows the fluctuating wind pressure coefficient. The absolute value is relatively large for a normalized diameter of 0.65. This is due to the separation, as mentioned earlier, and the other areas have similar values.

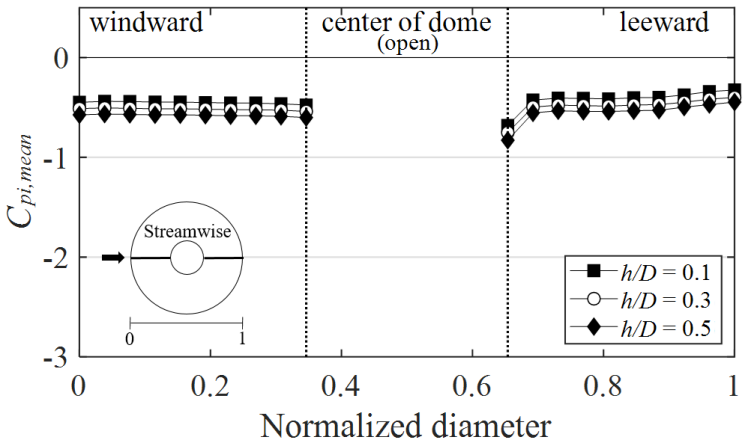

(a) $C_{pi,mean}$

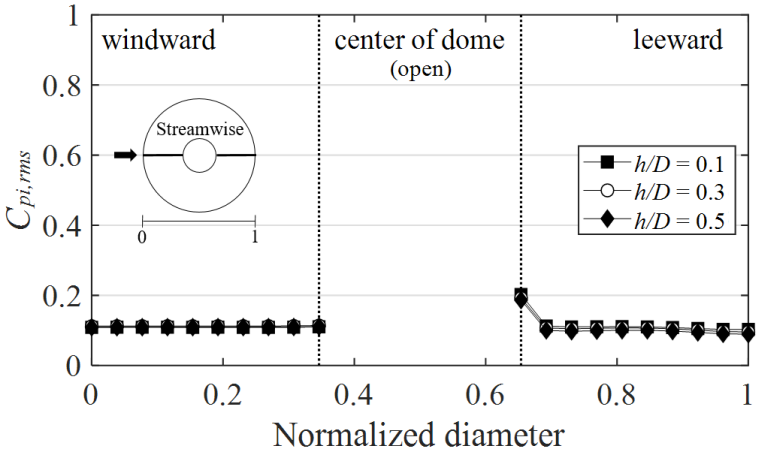

(b) $C_{pi,rms}$

Fig. 3.2 Variation of mean and fluctuating pressure coefficient for the internal roof surface of Model I

Fig. 3.5 shows the mean net pressure coefficient of Model I. For comparison, the mean pressure coefficient of the external roof is also plotted as a dotted line. Compared to the mean pressure coefficient for the external roof, it can be seen that the positive pressure is affected in the area not affected by separation. A positive net pressure implied that the load acted downward. This phenomenon is due to the fact that the negative pressure acting on the internal roof reduces the negative pressure generated on the external roof and increases the effect of positive pressure. However, at the roof edge of the open area, the mean net pressure coefficient was close to zero because the effects of separation occurring at the external and internal roofs in that area offset each other. Additional information regarding peak pressure coefficients is provided in Section 3.2.

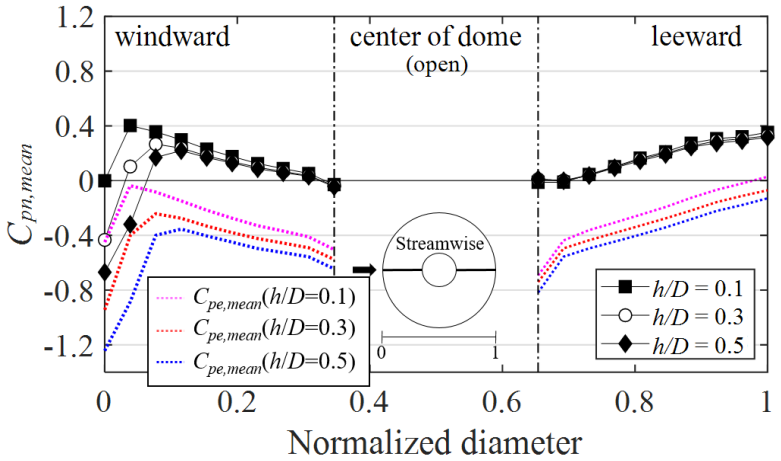

Fig. 3.5 Mean net pressure coefficient of Model I

3.2 Comparison of wind pressure coefficients depending on various wind environments

The results of previous studies showed that in the case of an enclosed dome roof, the positive pressure increased significantly in the windward area of the external roof owing to the increasing turbulence intensity with an increase in the power-law exponent, but the negative pressure was not significantly affected.

For the center-open dome roof, which is the target of this study, the tendency of the positive pressure to increase in the windward area of the external roof as the power-law exponent increased was the same as that of the closed dome roof. However, when the roof was opened, the negative pressure tended to increase in the leeward area of the external roof and all areas of the internal roof compared to that of the closed dome roof. Because all four models exhibited similar trends, this report presents representative graphs of the peak pressure coefficient and peak net pressure coefficient for Model I.

Fig. 3.6 shows a graph comparing the peak pressure coefficients for various power-law exponents. In Fig. 3.6(a), the negative peak pressure coefficient of the external roof shows very similar values for power-law exponents of 0.10 and 0.20, but there is an overall increase in the value of the power-law exponent of 0.27. Additionally, the increase is relatively large in the leeward area. Fig. 3.6(b) shows the positive peak pressure coefficient for the external roof. The positive peak pressure coefficient shows very similar values for power-law exponents of 0.10 and 0.20, but the absolute value of the power-law exponent of 0.27 shows an overall increasing trend. This increase was relatively large in the windward area.

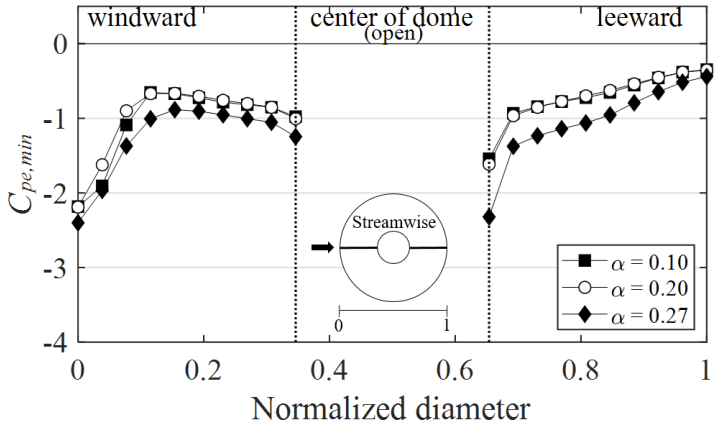

(a) $C_{pe,min}$

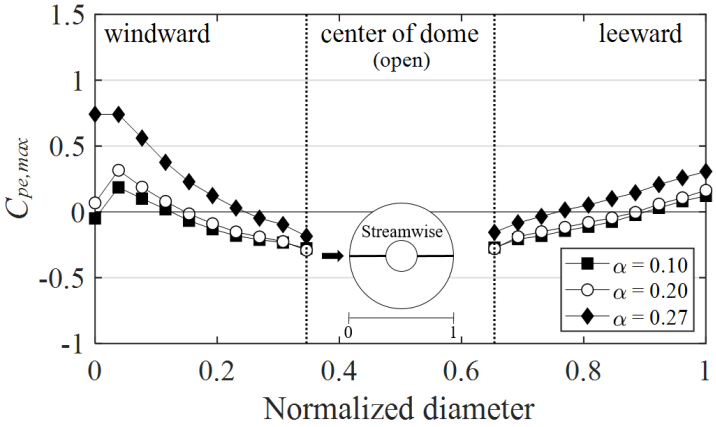

(b) $C_{pe,max}$

Fig. 3.6 External peak pressure coefficient depending on α of Model I

Fig. 3.7 shows the negative peak pressure coefficient for the internal roof. No positive peak pressure was observed on the internal roof; therefore, only a negative peak pressure was observed. Similar to the external roof, negative peak pressure showed a relatively large absolute value of the power-law exponent of 0.27. It is expected that as the negative pressure on the external roof increases, the negative pressure on the internal roof also increases.

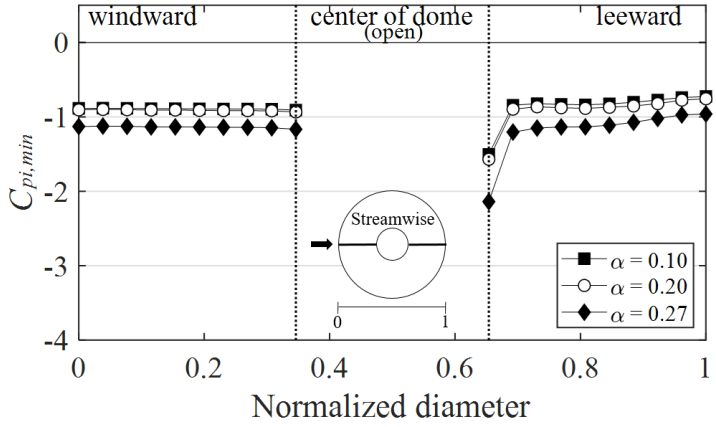

Fig. 3.7 Internal negative peak pressure coefficient depending on α of Model I (h/D=0.3)

To compare the peak pressure coefficient as the power-law exponent changes, the values for each model are listed in Tables 3.1–3.3. The values are representative of the values at the pressure taps located at the roof edges of the windward side and open area, where the absolute values are the largest along the center line. The locations of the pressure taps are shown in Fig. 3.8.

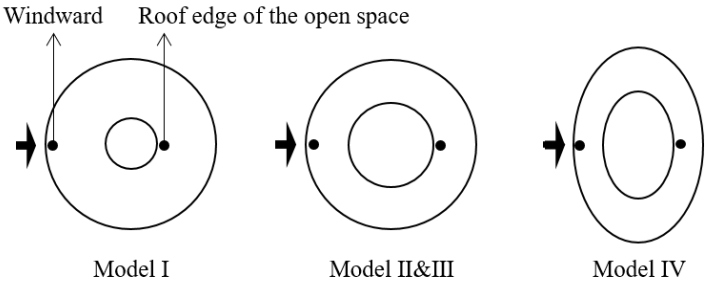

Fig. 3.8 Location of selected pressure tap

Table 3.1 External positive peak pressure coefficient on windward area(h/D=0.3)

α	Model Ⅰ	Model Ⅱ	Model Ⅲ	Model Ⅳ (90 °)
0.10	0.2	0.2	0	0.2
0.20	0.3	0.3	0	0.3
0.27	0.8	0.9	0.3	0.9

Table 3.2 External negative peak pressure coefficient on windward area(h/D=0.3)

α	Model Ⅰ	Model Ⅱ	Model Ⅲ	Model Ⅳ (90 °)
0.10	-1.5	-2.0	-1.5	-2.1
0.20	-1.7	-2.2	-1.7	-2.4
0.27	-2.3	-3.1	-2.0	-3.2

Table 3.3 Internal negative peak pressure coefficient at the roof edge of open area(h/D=0.3)

α	Model Ⅰ	Model Ⅱ	Model Ⅲ	Model Ⅳ (90 °)
0.10	-1.5	-2.0	-1.4	-1.8
0.20	-1.6	-1.9	-1.7	-1.8
0.27	-2.1	-3.0	-2.1	-2.3

As shown in Tables 3.1–3.3, the positive pressure increases in the windward area of the external roof, and the negative pressure increases in the leeward area of the external roof and all areas of the internal roof as the power-law exponent increases.

To confirm the effect of the increase in the peak pressure coefficient on the change in the peak net pressure coefficient, all models were examined, and the absolute value of the peak net pressure coefficient tended to increase as the power-law exponent increased. Particularly, the absolute value of the positive peak net pressure coefficient, which is the downward pressure, increased significantly in all areas owing to the increase in the negative pressure on the internal roof. However, the negative peak net pressure coefficient, which is the upward pressure, exhibits a relatively small increase in absolute value because the negative pressures on the external and internal roofs offset each other. This trend can be seen in Fig. 3.9.

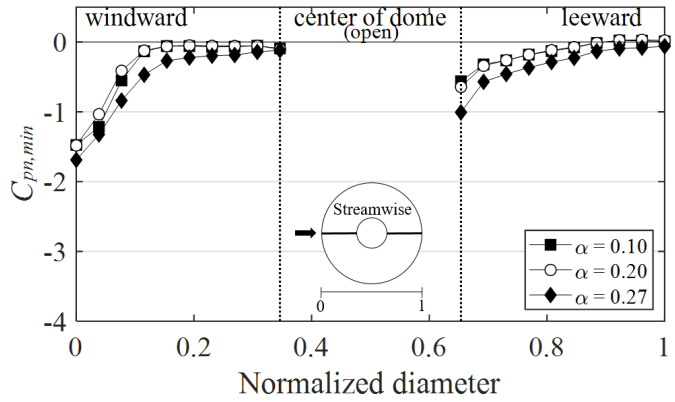

(a) $C_{pn,min}$

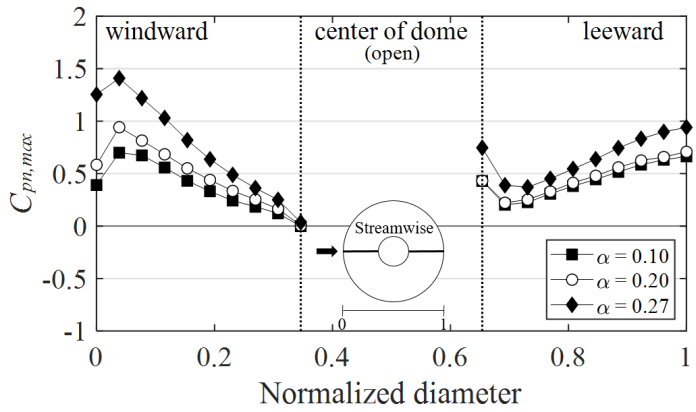

(b) $C_{pn,max}$

Fig. 3.9 Peak net pressure coefficient depending on α of the model I (h/D=0.3)

To compare the peak net pressure coefficient as the power-law exponent changes, the values for each model are listed in Tables 3.4–3.5. The locations of the pressure taps are shown in Fig. 3.8.

Table 3.4 Peak net pressure coefficient at the roof edge of windward area(h/D=0.3)

α	Model Ⅰ		Model Ⅱ		Model Ⅲ		Model Ⅳ (90 °)	
	$C_{pn,min}$	$C_{pn,max}$	$C_{pn,min}$	$C_{pn,max}$	$C_{pn,min}$	$C_{pn,max}$	$C_{pn,min}$	$C_{pn,max}$
0.10	-1.4	0.7	-1.4	0.7	-2.1	0.1	-1.5	0.8
0.20	-1.5	0.9	-1.6	0.9	-2.5	0.2	-1.4	1.1
0.27	-1.7	1.4	-1.8	1.4	-3.0	0.5	-1.9	1.6

Table 3.5 Peak net pressure coefficient at the roof edge of open area (h/D=0.3)

α	Model Ⅰ		Model Ⅱ		Model Ⅲ		Model Ⅳ (90 °)	
	$C_{pn,min}$	$C_{pn,max}$	$C_{pn,min}$	$C_{pn,max}$	$C_{pn,min}$	$C_{pn,max}$	$C_{pn,min}$	$C_{pn,max}$
0.10	-0.6	0.4	-1.1	0.7	-0.8	0.8	-0.9	0.8
0.20	-0.6	0.4	-1.4	0.7	-1.0	1.0	-1.1	0.9
0.27	-1.0	0.8	-1.8	1.2	-1.5	1.4	-1.9	1.1

3.3 Conclusions

In this study, wind pressure characteristics in various wind environments were analyzed for four central open-dome roofs of different shapes. The results are summarized as follows:

Based on previous studies of closed-dome roof, only the positive pressure in the windward area increases as the power-law exponent (α) increases. However, in the case of the central open dome roof, the positive and negative pressures in the windward and leeward areas of the external roof increased. As mentioned above, as the power-law exponent increases, the central open-dome roof increases the positive pressure in the windward area of the external roof and the negative pressure in the leeward area and in all areas of the internal roof. Therefore, in all areas of the external and internal roofs, the absolute value of the peak pressure coefficient tended to increase compared to that of the closed dome roof. Furthermore, these results indicate a large increase in the absolute value of the positive peak net pressure coefficient.

4. Published Paper etc.

[Underline the representative researcher and collaborate researchers]
[Published papers]

1. Cheon, DJ. Study on Wind Load for Designing Cladding of Retractable Dome Roof based on Wind Tunnel Test, Ph.D. Thesis, Seoul National University of Science and Technology, Seoul, Korea, 2023.

[Presentations at academic societies]

1. Cheon, D.J, Kim, Y.C, Yoon S.W, Wind Pressure Characteristics of Large-Space Roof Structures depending on Ground Surface Roughness, General Assembly, Spring Annual Conference of AIK, 2023

[Published books]

[Other]
Intellectual property rights, Homepage etc.

5. Research Group

1. Representative Researcher
Professor Sung Won, Yoon

2. Collaborate Researchers
Professor Yong Chul, Kim

Ph.D. Jong Ho, Lee

Ph.D. Dong Jin, Cheon

6. Abstract (half page)

Research Theme

Wind pressure characteristics of retractable dome roofs depending on various wind environments

Representative Researcher (Affiliation)

Professor **Sung Won, Yoon**

Seoul National University of Science and Technology

Summary・Figures

There are relatively fewer studies on wind load for retractable dome roofs than for general dome roofs, and a wind load code has yet to be established. Previous studies have focused on the shape of the roof, the retractable type, the opening ratio, the height-span ratio, and the rise-span ratio. However, in the previous research, only one airflow condition corresponding to power law exponent(α) = 0.15 of the Japanese wind load code was considered. The distribution of wind pressure on a dome roof varies according to the changes in velocity and turbulence intensity, which are characteristics of airflow. Therefore, in order to investigate the wind pressure characteristics of retractable dome roofs under various wind environments, this study analyzed the wind pressure characteristics of a central open dome roof according to three different power law exponents. As the power-law exponent increases, the central open-dome roof increases the positive pressure in the windward area of the external roof and the negative pressure in the leeward area and in all areas of the internal roof. Furthermore, these results indicate a large increase in the absolute value of the positive peak net pressure coefficient.